AIP | Journal of Applied Physics

Development of a passive and remote magnetic microsensor with thin-film giant magnetoimpedance element and surface acoustic wave transponder

H. Al Rowais, B. Li, C. Liang, S. Green, Y. Gianchandani et al.

Citation: J. Appl. Phys. 109, 07E524 (2011); doi: 10.1063/1.3562041
View online: http://dx.doi.org/10.1063/1.3562041
View Table of Contents: http://jap.aip.org/resource/1/JAPIAU/v109/i7
Published by the AIP Publishing LLC.

Development of a passive and remote magnetic microsensor with thin-film giant magnetoimpedance element and surface acoustic wave transponder

H. Al Rowais,[1,a)] B. Li,[1] C. Liang,[1] S. Green,[2] Y. Gianchandani,[2] and J. Kosel[1,b)]
[1]*Physical Sciences and Engineering Division, King Abdullah University of Science and Technology, 4700 KAUST, Thuwal 23955, Saudi Arabia*
[2]*Department of Electrical Engineering and Computer Science, University of Michigan, Ann Arbor, Michigan 48109, USA*

(Presented 17 November 2010; received 24 September 2010; accepted 8 December 2010; published online 5 April 2011)

This paper presents the development of a wireless magnetic field sensor consisting of a three-layer thin-film giant magnetoimpedance sensor and a surface acoustic wave device on one substrate. The goal of this integration is a passive and remotely interrogated sensor that can be easily mass fabricated using standard microfabrication tools. The design parameters, fabrication process, and a model of the integrated sensor are presented together with experimental results of the sensor.
 [doi:10.1063/1.3562041]

I. INTRODUCTION

Magnetic field sensors represent one of the most pervasive types of sensors today in e.g. automotive applications and process control, and they are becoming increasingly important in other fields like biomedical applications and communication electronics. In an attempt to improve the performance of magnetic sensors, various physical principles have been exploited.[1,2] Within those, the giant magnetoimpedance (GMI) effect is considered to offer great potential for a new generation of magnetic microsensors due to its high sensitivity to magnetic fields. The GMI effect is most effectively exploited in Co-based, amorphous wires,[3–5] which have proven to be good candidates for magnetic microparticle detection.[6] GMI thin film sensors have also been reported, but with less sensitivity than their wire counterparts.[7,8]

GMI sensors change their impedance as a function of an external magnetic field due to the skin effect at high frequencies. The operation frequency lies in the MHz range, which provides both the option to boost sensor signals due to resonance effects and the option to combine the sensor with an RF transducer. In this case, passive and remote sensors can be realized providing more flexibility for magnetic sensing applications in harsh conditions, on rotating or moving parts, for nondestructive testing, and in encapsulated environments. Previously, such a sensor has been developed utilizing a GMI wire and a surface acoustic wave (SAW) transponder.[9] The SAW transponder is a two-port device that utilizes the dependency of the acoustic reflection on the electrical load at one of its ports.

This study reports the development of a magnetic field microsensor consisting of the novel combination of a thin-film GMI element and a SAW transponder, which are integrated on a lithium niobate ($LiNbO_3$) substrate. This is the first step toward a wirelessly interrogable, integrated and passive magnetic sensor, which can be produced by means of batch fabrication.

II. METHOD

A. Concept

Figure 1 shows the overall design concept of the sensor. The proposed integrated sensor is interrogated wirelessly through the dipole antenna that is attached to the source interdigital transducer (IDT1). IDT1 sends Rayleigh waves through the piezoelectric substrate, which are reflected off the reference IDT (IDT2) and the load IDT (IDT3). IDT3 is connected to a three-layer thin film GMI element, which is fabricated on the same $LiNbO_3$ substrate as the IDTs. IDT1 sends the signals back to the interrogator to extract the sensor information from the difference in phase and magnitude of the reflections of IDT2 and IDT3.

B. GMI sensor

The three-layer sensor was composed of two soft magnetic $Co_{73}Si_{12}B_{15}$ layers, each 1 μm in thicknesses, and

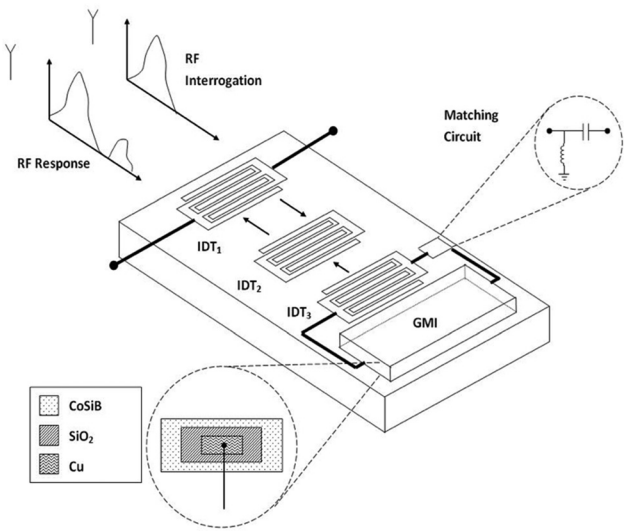

FIG. 1. Schematic of the principle of operation of the wireless sensor device.

a)Electronic mail: hommood.alrowais@kaust.edu.sa.
b)Electronic mail: jurgen.kosel@kaust.edu.sa.

a 0.5 μm thick layer of copper. The dimensions of the sensor were 3000 μm by 200 μm.

C. SAW transponder

The piezoelectric substrate chosen for this application was lithium niobate ($LiNbO_3$) (128 deg Y-X cut), and the IDTs were made of copper. The dimensions are inversely proportional to the center frequency f_0, which was chosen to be 80 MHz:

$$f_0 = \frac{v}{d}, \tag{1}$$

where v is the Rayleigh wave velocity, which is 3488 m/s for $LiNbO_3$, and d is the periodicity of the IDTs. The number of the finger pairs (N) in the IDT inversely affects the bandwidth (BW) of the transducer:

$$\mathrm{BW} = \frac{\alpha f_0}{N}, \tag{2}$$

where α is constant factor. From Eq. (1) and Eq. (2), and a BW of 20 MHz the dimensions of the IDTs were evaluated as follows: $d = 50$ μm, $N = 20$, and the finger width was set at 12.5 μm. The spacing (w) between the three IDTs was 1250 μm to provide a time-shift between the responses of IDT2 and IDT3 of

$$\Delta t = \frac{v}{w} = 0.36\,\mu s. \tag{3}$$

The thickness of the IDTs was 120 nm. The electrical impedance of the IDT was experimentally found to be 10 Ωs. The finger length should be at least 30 times the periodicity so as to not cause diffraction[10] and was chosen to be 1500 μm.

D. Circuits

The GMI sensor is part of a series resonant circuit (Fig. 2) in order to maximize the sensitivity. The resonant circuit is made of the GMI element connected to a capacitor in series. The value of the capacitor was evaluated based on the calculation of the resonant frequency (ω):

$$\omega = \frac{1}{\sqrt{C_R L_G}}, \tag{4}$$

where C_R is the capacitance and L_G is the inductance of the GMI element. The inductance of the GMI sensor without external magnetic field was found to be $L_G = 8$ nH. Therefore, a value of $C_R = 500$ pF was required for a center frequency of 80 MHz. The design of the capacitance was a longitudinal (comb drive) capacitor that showed a finger overlap of 1000 μm, finger length of 1000 μm, spacing of 10 μm, and five fingers. An impedance matching circuit, implemented by L_M and C_M (Fig. 2) ensures optimal transfer of power to the GMI load.

E. Fabrication

The fabrication of the integrated device was accomplished in several steps as shown in Fig. 3. First, a 3 μm thick

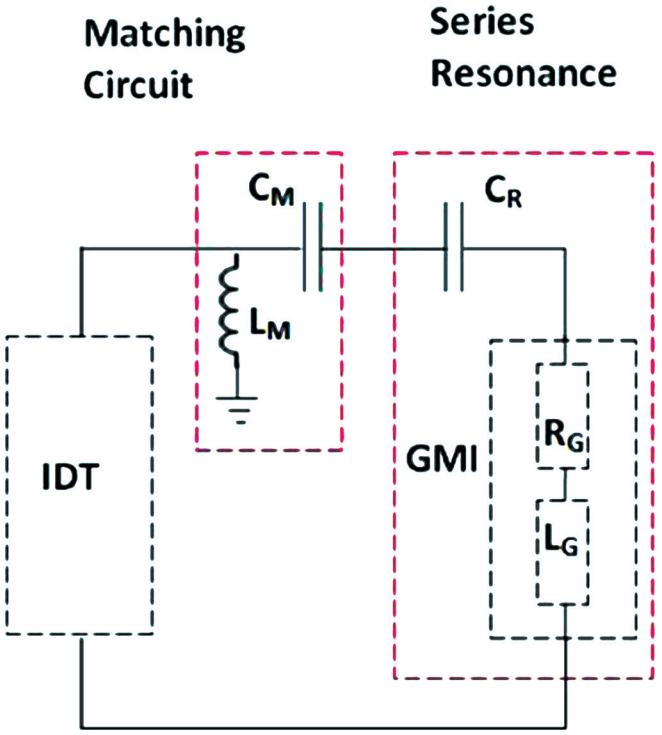

FIG. 2. (Color online) Matching circuit and series resonance circuit.

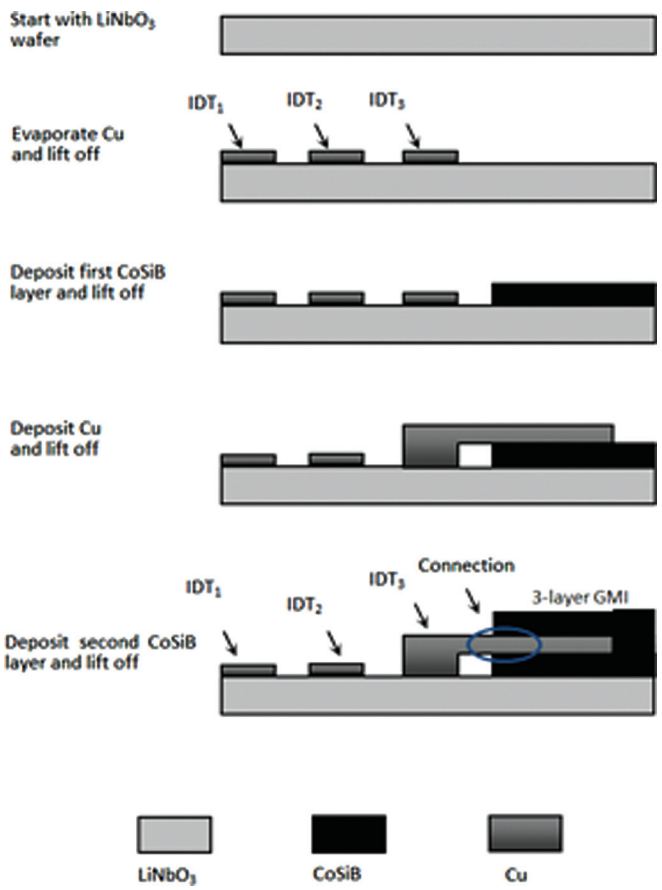

FIG. 3. (Color online) Fabrication process of the integrated sensor.

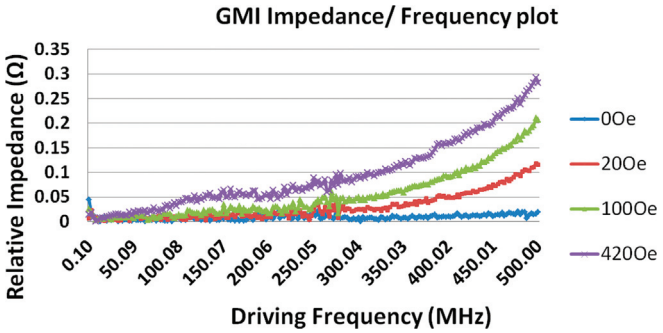

FIG. 4. (Color online) Impedance magnitude of the GMI sensor as a function of the frequency of the measurement current under different external magnetic fields.

photoresist (SPR 220) was spin-coated, exposed to UV light and developed to provide pattern for the IDT structures. Then, a copper layer of 120 nm in thickness was deposited by evaporation followed by a lift-off process. For the fabrication of the GMI sensor AZ 9260 photoresist was used providing a 6 μm thick layer. The deposition of the magnetic material was accomplished by dc sputtering (base pressure: 2×10^{-6} Torr, Ar flow pressure: 7 mTorr, sputtering power: 250 W). During the deposition, a dc magnetic field of 500 Oe was applied parallel to the desired easy axis of the GMI sensor. The composition of the CoSiB layer was analyzed by means of XPS, and found to be 73/12/15 at. %. After the fabrication of the first magnetic layer, similar photolithography steps were applied to fabricate the copper layer and the second magnetic layer. Finally, the device was subjected to field annealing at 300 °C with a constant magnetic field of 1500 Oe in the desired easy direction of the magnetic layers.

III. RESULTS

First, the GMI sensor was tested separately. The impedance magnitude of the GMI element was measured by using an Agilent 4395A Network/Spectrum/Impedance Analyzer with an Agilent 43961A RF impedance test kit installed The calibration was done using the GMI sensor at zero applied field, hence, the impedance data collected was relative to the zero field impedance of the sensor. Figure 4 shows the impedance magnitude of the GMI sensor as a function of the frequency for values of H_{ext} of 0, 20, 100, and 420 Oe. The magnitude of the impedance increases monotonically along with the frequency and the magnetic field. Figure 5 shows the loaded IDT with a GMI sensor element and the series resonance capacitor fabricated on the $LiNbO_3$ wafer.

IV. CONCLUSION

A fully integrated magnetic field sensor was designed consisting of a GMI sensor and a SAW transducer. A fabrication process was developed to integrate a three-layer GMI sensor on a $LiNbO_3$ substrate together with the interdigital transducers of the SAW transponder and a comb-finger capacitor. The response of the fabricated GMI sensor to an applied external magnetic field was evaluated, showing an impedance magnitude increase of 0.3 Ωs at a frequency of 500 MHz at 420 Oe. Future work will focus on testing the fully integrated device—including the response of the SAW and the performance of an RF antenna—and improving the response of the GMI sensor.

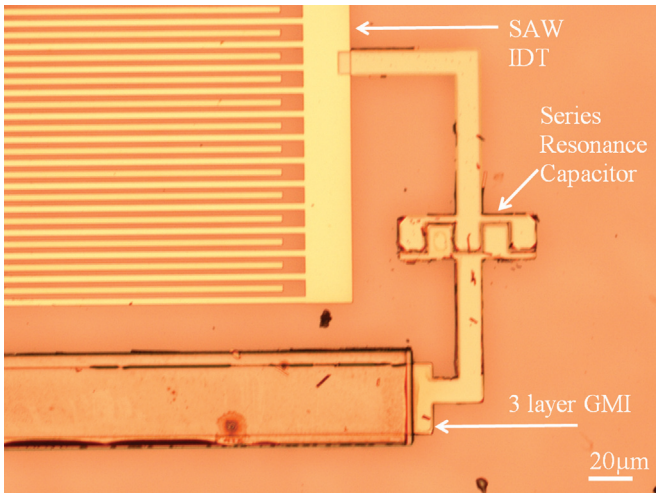

FIG. 5. (Color online) Optical microscopic picture of the IDT of the SAW transponder, the GMI sensor element and the comb capacitor.

ACKNOWLEDGMENTS

This work was performed in part at the Lurie Nanofabrication Facility at the University of Michigan, a member of the National Nanotechnology Infrastructure Network, which is supported in part by the National Science Foundation.

[1]J. Lenz and A. S. Edelstein, IEEE Sens. J. **6**, 631 (2006).
[2]A. E. Mahdi, L. Panina, and D. Mapps, Sens. and Actuators, A **105**, 271 (2003).
[3]L. V. Panina and K. Mohri, Appl. Phys. Lett. **65**, 1189 (1994).
[4]M. Vazquez, J. M. Garcıa-Beneytez, and J. P. Sinnecker, J. Appl. Phys. **83**, 6578 (1998).
[5]C. Garcia, A. Zhukov, J. Gonzalez, V. Zhukova, and J. Blancoe, J. Opt. Adv. **8**, 1706 (2006).
[6]H. Chiriaca, D. Herea, and S. Corodeanu, J. Magn. Magn. Mater. **311**, 425 (2007).
[7]I. Giouroudi, H. Hauser, L. Musiejovsky, and J. Steurer, J. Appl. Phys. **99**, 08D906 (2006).
[8]W. Wang, Thin Solid Films **484**, 299 (2005).
[9]H. Hauser, R. Steindl, C. Hausleitner, A. Pohl, and J. Nicolics, IEEE Trans. Instrum. Meas. **49**, 648 (2000).
[10]D. Ballantine, R. White, S. Martin, A. Ricco, E. Zellers. G. Frye, and H. Wohltjen, *Acoustic Wave Sensors: Theory, Design and Physico-Chemical Applications* (Academic, San Diego, 1997), Chap. 6.